Flexible hinge-based antenna pointing mechanism

Sachin Barthwal[1], Manish Trikha[2], Ashitava Ghosal [3]

[1] U R Rao Satellite Centre, Bangalore, 560017, India, sachinb@ursc.gov.in
[2] Human Space Flight Centre, ISRO, Bangalore, 560094, India,
mtrikha-hsfc@isro.gov.in
[3] Department of Mechanical Engineering, IISc, Bangalore, 560012, India,
asitava@iisc.ac.in

Abstract. A flexure-based three-degree of freedom (two rotations and one translation) is studied in this paper for application in an antenna pointing mechanism (APM). The antenna is rigidly connected to the moving platform of the manipulator. The platform is supported by three symmetrically arranged legs, and each leg has a revolute(R)-prismatic(P)-spherical(S) joint configuration. The inverse kinematics (IK) of the three legs in the 3-RPS parallel manipulator is used to compute the angles in the passive R and S joints and the translation at the prismatic P joints for a desired rotation of the antenna about two axes. These results are then used to design flexure hinges, which replace the revolute and spherical joints without any loss of orientation capability of the moving platform. The design parameters of the manipulator and flexure hinge are verified by the analysis, and numerical results are provided.

Keywords: 3-RPS, flexure joint, antenna pointing mechanism.

1 Introduction

Antenna pointing is the process of adjusting an antenna's azimuth, elevation, and polarizing angles for transmitting or receiving electromagnetic signals. There are several different types of antennas, and in this work, we consider a commonly used reflector type of antenna that requires an antenna pointing mechanism (APM) for pointing the antenna in a desired direction. If the antenna pointing vector is not in the line of sight, it is called a pointing error, and a pointing error leads to degradation of the performance of the antenna. An antenna can be mounted in different configurations depending on the tracking requirements; a few among them are azimuth over elevation mount, X-Y axes mount, and polar mount.

In azimuth over elevation configuration, the antenna is mounted along two axes where the supporting structure element is perpendicular to rotating the rotating axis. The arrangement can be thought of as a serial chain with two revolute (R) joints in series -- the rotation of one of the R joints changes the azimuthal angle, whereas rotation along the other R joint changes the elevation angle. This type of mount covers almost all regions in space except the space directly overhead of the azimuth axis. The main source of errors in the azimuth over-elevation mounting arrangement are the errors in the joints, and since it is a serial arrangement, the final pointing error is the sum of the

errors at the joints. It is well known that in a parallel manipulator, the maximum error in the moving platform is the maximum error in the chain connecting the moving platform to the fixed base. Thus, the error is expected to be less than in a serial arrangement. However, in a parallel configuration, there may be more than one passive joint, and the passive joints' errors will affect the pointing accuracy.

Gough was the first to introduce a six-degree of freedom (DOF) parallel manipulator for tire testing applications, and later, it was used for motion simulators by Stewart. However, 6 DOF are not required for antenna pointing, and in this work, we propose a 3 DOF parallel manipulator for this application.

Although parallel manipulator has many advantages, one of the main issues is the presence of passive joints. Eliminating errors at passive joints due to joint clearances, friction, and unmodeled dynamics is challenging due to the low repeatability and randomness of errors [1]. Since the major source of error in parallel manipulators is joint clearance, it becomes necessary to eliminate these for high-accuracy pointing applications. These errors can be avoided by replacing clearance-affected joints with flexure-based joints [2]. A flexure joint has many advantages, such as high repeatability, no backlash, no lubrication requirement, and no hysteresis. Parallel manipulators with flexure joints have been studied by various researchers for high-accuracy micro-manipulations [3], [4], [5]. In flexure-based parallel manipulators, the passive joints are replaced with compliant hinges; this avoids the problem encountered in conventional joints. Once the geometric configuration of flexure hinges is finalized, the relation between load and displacement is used for the kinematic modeling of the mechanism.

Ryu et al. [6] studied the kinematics of flexure hinge-based parallel manipulators using the stiffness model. The manipulator under consideration had a maximum rotation range of 322.8 arcsecs and movement of 41.5 and 47.8 micrometers along the X and Y axes. Yu et al. [7] studied the 3-RRPR flexure-based parallel manipulator for bioengineering applications with a translational range of 71.28 and 71.02 micrometers along the X and Y axes. The flexure hinge is designed for minimum generated stress over working ranges for the maximum number of working cycles. This limits the use of hinges for manipulators with large strokes or heavy-duty working cycles.

The flexure hinges are either optimally designed or assembled in group configurations to overcome these constraints. For large strokes, flexible hinges can be designed by increasing the extension of the deformable material. However, this results in a significant drift of the axis of rotation. Designing the flexure hinge with high rotation accuracy for large deflections is challenging. Many novel approaches were carried out to design for this objective. Robert et al. [8] designed a large displacement monolithic compliant rotation hinge for rotation up to 90°. Pengbu et al. [9] proposed a helix-based revolute flexure hinge with the large stroke of ± 150° with zero axis drift. Naves et al. [10] proposed a large stroke three DOF spherical flexure joint with a capacity up to 30°. These existing works give us motivation and confidence in using compliant hinges for

higher stroke applications. A literature survey on complaint hinge-based parallel manipulators (CHBPM) reveals that there is very little research on CHBPM for larger platform rotation and actuation. In this work, we attempt to study the CHBPM pointing application for a rotation range of ± 10° of the platform along the X and Y axes.

2 Modeling of 3-RPS parallel manipulator

In this work, we propose to use the well-known 3-RPS parallel manipulator – R, P, and S denote a rotary, prismatic, and spherical joint, respectively. A schematic of the 3-RPS parallel manipulator is shown in Fig. 1 where A_1, A_2, and A_3 are the S joints, B_1, B_2, and B_3 are the R joints, and the translation at the P joints are denoted by L_i ($i \in 1,2,3$). The 3-RPS parallel manipulator has three degrees of freedom – it can rotate about two axes, namely X and Y, and translate along the third Z-axis [11]. In this work, we keep the Z motion constant and use the two rotations about X and Y axis for antenna pointing – similar to the work described in Ashith et al. [12].

The (top) moving platform is supported by three legs which are 120° apart from each other. Each leg is of RPS configuration. The revolute joint is connected to the base (bottom platform), and the spherical is connected to the moving platform.

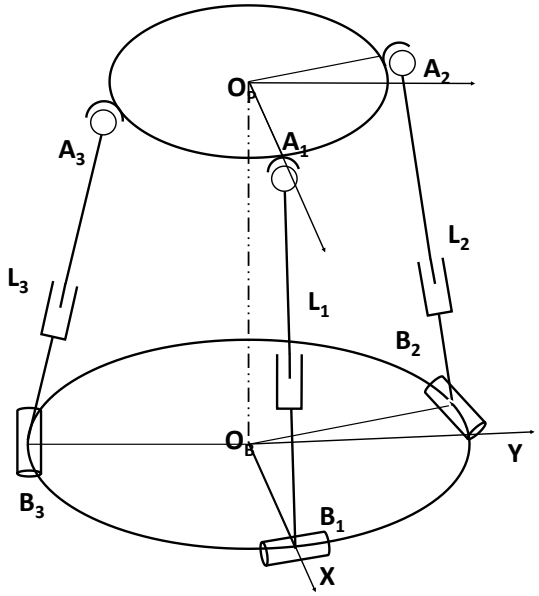

Fig. 1. Schematic of a 3-RPS Manipulator

To study the spherical joint more conveniently, we model a spherical joint as three revolute joints mutually perpendicular and intersecting at a point [13]. Four consecutive Euler rotations, Z-Y-X (or 321) of the rotary joint while moving from leg to platform gives the equivalent movement as that of a spherical joint. The equivalent Denavit - Hartenberg (D-H) table for a spherical joint is given below.

Table 1. DH Parameters for a spherical joint.

i	α_{i-1}	a_{i-1}	d_i	θ_i
1	0	0	0	θ_{s1}
2	- $\pi/2$	0	0	$\theta_{s2} + \pi/2$
3	- $\pi/2$	0	0	$\theta_{s3} + \pi/2$
4	- $\pi/2$	0	0	- $\pi/2$

The location of B_i and A_i ($i \in 1,2,3$). with respect to their reference to the frame can be written as

$$A_i = [a\cos(\phi) \quad a\sin(\phi) \quad 0]^T$$
$$B_i = [b\cos(\phi) \quad b\sin(\phi) \quad 0]^T$$

where ϕ is the orientation angle of the leg with respect to leg-1, b is the radius of the triangular circumscribed base circle, and a is the radius of the triangular circumscribed platform circle.

The position of spherical joints, A_i, with respect to the frame XYZ, can be expressed by

$$\begin{bmatrix} a_i \\ 1 \end{bmatrix} = \begin{bmatrix} R & p \\ 0 & 1 \end{bmatrix} . \begin{bmatrix} a_i \\ 1 \end{bmatrix} = [T] . \begin{bmatrix} a_i \\ 1 \end{bmatrix} \quad , i = 1,2,3$$

The homogeneous transformation $[T]$ matrix relates the moving coordinate frame O_P-xyz with the fixed coordinate frame O_B-XYZ given by

$$[T] = \begin{bmatrix} C\beta C\gamma & -C\beta S\gamma & S\beta & x_T \\ S\alpha S\beta C\gamma + C\alpha S\gamma & -S\alpha S\beta S\gamma + C\alpha C\gamma & -S\alpha C\beta & y_T \\ C\alpha S\beta C\gamma + C\alpha C\gamma & C\alpha S\beta S\gamma + S\alpha C\gamma & C\alpha C\beta & z_T \\ 0 & 0 & 0 & 1 \end{bmatrix}$$

where the position vector of origin (center of platform) of the frame xyz is given by $[x_T \quad y_T \quad z_T]^T = p$ with respect to fixed coordinate frame XYZ. The Euler angles (ZYX type) of moving platform are $\alpha, \beta, \& \gamma$,.Where $S\alpha, S\beta, S\gamma, C\alpha, C\beta, C\gamma,$ indicate Sinα, Sin β, Sin γ, Cos α, Cos β and Cos γ, respectively. The mechanism consists of three parallel loops. Each loop forms a vector chain of links as shown in Fig 1. The equation in vector form can be written as

$$\mathbf{L_i} = \mathbf{a_i} + \mathbf{p} - \mathbf{b_i} \qquad (1)$$

where $L_i (i \in 1,2,3)$ is the position vector for each leg.

The inverse kinematic analysis, performed using eq. (1), is done to measure the actuation for a given platform posture [14]. A numerical study was carried out for a platform configuration of the b =20 cm, a = 10cm and platform height (z_T) =31cm. Once the position and orientation of the moving platform are prescribed, the actuations, L_i =1,2,3 (see Fig. 1) can be found, and the angles at the S and R passive joints can be calculated by using D-H parameters for each leg [15]. The rotations at the R and S joint for ± 10° along X and Y axis for the moving platform are shown in Table 2.

Table 2. Joint angles in a 3-RPS manipulator from IK.

Joint	Axis	Range of angle (degrees)	Total angle (degrees)
S_1	Yaw	0 to 1	1
	Pitch	-10.25 to 10.09	20.34
	Roll	-9.90 to 10.01	19.91
S_2	Yaw	0 to 1.4	1.4
	Pitch	-10.5 to 10.90	21.40
	Roll	-11.99 to 10.30	22.29
S_3	Yaw	0 to 0.92	0.92
	Pitch	-9.4 to 9.5	18.9
	Roll	-10.3 to 9.90	20.20
R_1	Yaw	-1 to 0.5	1.5
R_2	Yaw	-1.90 to 0.5	2.4
R_3	Yaw	-0.18 to 0.8	0.98
where L_1 = 30.5 to 34.9 cm , L_2 = 30.39 to 34.9 cm and L_3 = 31.8 to 33.5 cm			

3 Design of 3-RPS parallel manipulator for APM

The design was carried out in three steps. First, the best possible configuration of a parallel manipulator for the lowest possible passive joint rotation was selected. Second, the compliant flexure hinge is designed for an observed range of angles and deflections. Third, the passive joints are replaced with designed flexure hinges, and multi-body simulation analysis is carried out for validation.

The observed angles at spherical joints are similar to platform rotations of ± 10°, while angles observed for revolute joints are small of the order of a few degrees. Hence, an attempt was made to design the flexure hinge, which can rotate ± 10° along X and Y axis and replaces the passive joints of the manipulator with the designed flexure hinges.

Flexure-based spherical joint uses folded leaf springs as a flexible connecting member to obtain the required degrees of motion. In these joints folded springs are connected between two ends of a joint in different topologies to get the required stiffness and rotation. Serial stacked folded leaf spring-based joint is selected as it has benign translational errors. One end of leaf springs is connected to one end of the joint and another to the middle ring. A schematic of the flexure hinge for a spherical joint is shown in Fig. 2.

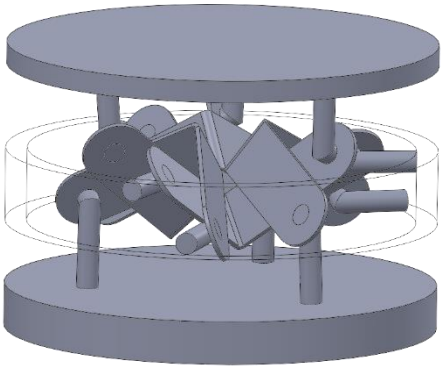

Fig. 2. Serial stacked spherical flexure hinge joint

The design methodology was validated by creating a 3D model of the 3-RPS manipulator in SolidWorks and ADAMS. The motion at the joints was obtained from the ADAMS and SolidWorks model for the required ± 10° rotations of the platform about two axes. The spherical and revolute joint angles calculated using the inverse kinematic (see Table 2) and from ADAMS are found to be consistent. These results give us confidence in the 3D SolidWorks model and for selecting and designing flexure hinges. The series of leaf hinges in a special configuration are chosen to replace the spherical joint, while the monolithic hinges replace the revolute joint. The arrangement of stacked leaf spring can be called as spherical flexure hinge (SFH). The dynamic analysis of SFH was carried out using ADAMS Flex for the deformations and stresses. Further, a complete dynamic analysis of compliant hinge based parallel manipulator (CHBPM) was carried out to obtain motion and forces experienced by the manipulator. This work is continuing.

4 Results

The motion analysis of the manipulator using ADAMS provided the range of angles turned by each joint in yaw, pitch, and roll directions for the platform rotation ± 10° motion along two axis. The maximum range of angle is observed at the spherical joint S2 and is about 22.71° along one axis and 21.22° along another. The height of the platform is kept constant and the actuation observed at prismatic joints is about 5 cm. These results match with observed outputs from DH method (Table-2).

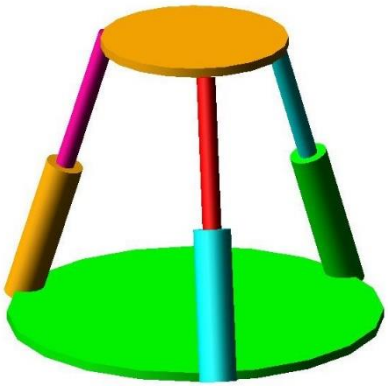

Fig. 3. ADAMS model of a 3-RPS manipulator

Table 3. Joint angles (ADAMS) observed in a 3-RPS manipulator.

Joint	Axis	Range of angle (degrees)	Total angle (degrees)
S_1	Yaw	0 to 1	1
	Pitch	-10.17 to 10.17	20.34
	Roll	-10.17 to 10.17	20.34
S_2	Yaw	0 to 1.2	1.2
	Pitch	-10.2 to 11.02	21.22
	Roll	-12.04 to 10.67	22.71
S_3	Yaw	0 to 0.97	0.97
	Pitch	-9.9 to 9.7	19.6
	Roll	-10.6 to 10.2	20.80
R_1	Yaw	-1.2 to 0.6	1.8
R_2	Yaw	-2.10 to 0.6	2.7
R_3	Yaw	-0.16 to 0.6	0.22
where L_1 = 30.9 to 34.3 cm , L_2 = 30.4 to 35.0 cm and L_3 = 31.9 to 33.1 cm			

The 3D modeling of hinge was carried out in SolidWorks and then imported to ADAMS. The leaf springs of SFH were converted into flexible elements using ADAMS Flex. The dynamic analysis of the SFH was carried out for a load of 50N acting downward, and for the motion of 23° range (± 11.5°) along two axes to the upper side of SFH keeping lower side fixed. The stresses observed in individual folded leaf springs are in the order of 600MPa, except few nodes due to stress localization at the constraints given between mating components. This is half of the yield stress for chosen material for the leaf spring and this gives us confidence on the possible replacement of passive joints with these SFHs.

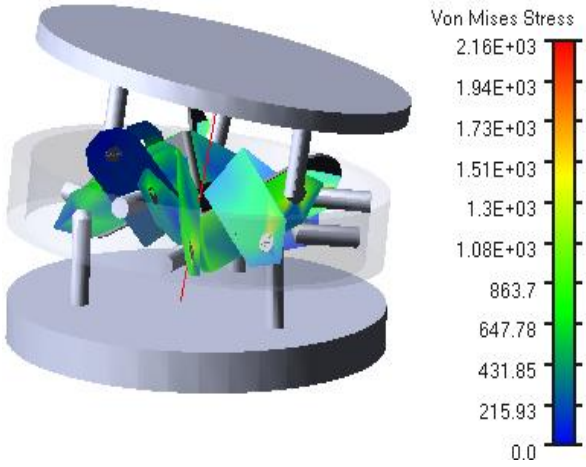

Fig. 4. Dynamic results of flexure based joint

5 Conclusion

This work deals with the modeling and design of a three-degree-of-freedom parallel manipulator, namely the 3-RPS parallel manipulator, for an antenna pointing mechanism. The antenna pointing mechanism is designed for ± 10° motion about two axes. To reduce the friction, backlash and other non-linear effects in kinematic (R and S) joint and to reduce unpredictable errors, flexible hinges are proposed used. The flexible hinges in the 3-RPS manipulator are designed to achieve the required rotations obtained from kinematic analysis. The designed flexural hinges are analyzed in multi-body software to ensure that the stresses are well within limits thus ensuring that they will not fail due to fatigue. This work is continuing and efforts are being made to refine the design, fabricate the antenna pointing mechanism and validate the design experimentally.

References

1. Meng, J., Zhang, D. and Z. Li, "Accuracy analysis of parallel manipulators with joint clearance," Journal of Mechanical Design, Vol. 131, no. 1, Pages 011013, 2009.
2. Howell, L.L., Magleby, S.P. and Olsen, B.M., ``Handbook of Compliant Mechanisms'', Wiley, New York (2013). ISBN 978-1-119-95345-6.
3. Gayral,T., Daney, D. and Ducarne, J., ``Flexure joints modeling for micrometer accuracy of an active 6-PUS space telescope through experimental calibration'', 2013 IEEE International Conference on Robotics and Automation (ICRA)Karlsruhe, Germany, May 6-10, 2013.

4. Dong, W., Du, Z. and Sun, L., ``Conception design and kinematics modeling of a wide-range flexure hinge-based parallel manipulator'', Proceedings of the 2005 IEEE International Conference on Robotics and Automation Barcelona, Spain, April 2005.
5. Du, Z., Shi, R. and Dong, W., "A piezo-actuated high precision flexible parallel pointing mechanism: Conceptual design, development, and experiments," IEEE Trans. Robot., vol. 30, no. 1, pp. 131–137, 2014.
6. Ryu, J. W., Lee, S.-Q., Gweon, D.-G. and Moon, K. S., "Inverse kinematics modeling of a coupled flexure hinge mechanism," Mechatronics, Vol. 9, pp.657-674, Sep. 1999.
7. Yu, J.J., Zong, G. H., Bi, S. S. and Zhao, W., "Design of a compliant manipulator with nanometer range resolution," Journal of Chinese Mechanical Engineering, Vol.13, pp.1577-1580, Sep. 2002.
8. Fowler, R. M, Maselli, A., Pluimers, P., Magleby, P. S. and Howell, L.L, ``Flex-16: A large-displacement monolithic compliant rotational hinge'', Mechanism, and Machine Theory, Volume 82, 2014, Pages 203-217.
9. Liu, P, Yao, G. and Yan, L., ``Design of a helix-based revolute flexure hinge with large stroke'', 2021 IEEE International Conference on Manipulation, Manufacturing and Measurement on the Nanoscale (3M-NANO), Xi'an, China, 2021, pp. 117-121, doi: 10.1109/3M-NANO49087.2021.9599828.
10. Naves, M., R.G.K.M. Aarts, R. G. K.M, Brouwer, D. M., ``Large stroke high off-axis stiffness three degree of freedom spherical flexure joint'', Precision Engineering, Volume 56, 2019, Pages 422-431.
11. Lee, K-M and Shah, D. K, "Kinematic analysis of a three-degrees-of-freedom in-parallel actuated manipulator." IEEE J. Robotics Autom. Vol. 4, 1988, Pages 354-360.
12. Ashith Shyam, R. B, Acharya, M., Ghosal, A., ``A heliostat based on a three-degree-of-freedom parallel manipulator'', Solar Energy, Volume 157, 2017, Pages 672-686,
13. Shah, S. & Saha, Subir & Dutt, Jayanta Kumar. (2012). Denavit-Hartenberg Parameterization of Euler Angles. Journal of Computational and Nonlinear Dynamics. 7. 021006. 10.1115/1.4005467.
14. Desai, R., Muthuswamy, S. A, ``Forward, inverse kinematics and workspace analysis of 3RPS and 3RPS-R parallel manipulators'', Iran J Sci Technol Trans Mech Eng 45, 115–131 (2021). https://doi.org/10.1007/s40997-020-00346-9
15. Ghosal A., Ashith Shyam, R. B., ``A three-degree-of-freedom parallel manipulator for concentrated solar power towers: Modeling, simulation and design'', AIP Conference Proceedings 31 May 2016; 1734 (1): 160006. https://doi.org/10.1063/1.4949247.
16. MSC Software ADAMS/View, Flex 2020, MSC Software Corporation, Newport Beach, California, USA.
17. SolidWorks Premium 2021, Dassault Syst´emes SolidWorks Corp., Waltham, MA, USA